Polarization Rotator in Low Index Contrast Substrates for Mid-Infrared Photonic Integration

Swapnajit Chakravarty[2], Jason Midkiff[2], Chi-Jui Chung[1], Ali Rostamian[1], Joel Guo[1], Ray Chen[1,2]
[1]Department of Electrical and Computer Engineering, University of Texas at Austin, 10100 Burnet Rd. Austin, TX 78758, USA
[2]Omega Optics, Inc., 8500 Shoal Creek Blvd., Bldg. 4, Suite 200, Austin, Texas 78757, USA
Author e-mail address: swapnajit.chakravarty@omegaoptics.com, chenrt@austin.utexas.edu

Abstract: We demonstrate polarization rotators in low index contrast InGaAs-InP material system to enable monolithic integration of quantum cascade lasers and detectors with slotted photonic crystal waveguide gas sensors in the molecular fingerprint region from λ=3-15μm.

In a typical photonic integrated circuit with an upper air cladding and a lower dielectric cladding, the transverse-magnetic (TM) polarized guided mode, with lower effective index, has higher bending loss than the transverse electric (TE) polarized guided mode, thereby necessitating larger bending radius of curvature for the TM mode than the TE mode. Particularly, in III-V integrated circuits where the wafer cost scales with epitaxial growth thickness, it is therefore necessary to efficiently utilize real estate on a chip. Quantum cascade lasers (QCLs) only emit in TM polarization. However, passive photonic devices such as photonic crystal waveguides when fabricated in the most common air holes in a dielectric slab configuration, can only support TE modes. In recent years, we have experimentally demonstrated that slotted photonic crystal waveguides can enable high sensitivity gas sensing on chip via absorption spectroscopy. We have shown detection of 3 parts per million (ppm) greenhouse gas carbon monoxide (CO) at λ=4.55μm with feasibility to detect down to sub-100 parts per billion (ppb) by nominal device modifications in a silicon-on-sapphire (SoS) platform [1]. We previously demonstrated the detection of the chemical warfare simulant triethylphosphate (TEP) down to 10ppm at λ=3.4μm also in a SoS platform [2]. An efficient TM to TE conversion device is thus desired. While CO has maximum absorbance at λ=4.55μm where SoS can be used as an available substrate with silicon core for low-loss waveguiding (~2dB/cm), silicon cannot be used at λ=9.5μm at the absorbance maxima of TEP. Available core-cladding choices such as Ge-GaAs, GaAs-AlGaAs, InGaAs-InP would need suspended membrane photonic crystal waveguide geometries. However, since the most efficient QCLs demonstrated till date are in the InP platform, the choice of InGaAs-InP eliminates need for wafer bonding versus other choices [3]. The InGaAs-InP material platform can also potentially cover the entire molecular fingerprint region from λ=3-15μm.

In this paper, we focus on the design, fabrication and characterization of polarization rotators in the low-index contrast InGaAs-InP material system. Our designs at the present time are centered on the ammonia absorbance peak at λ=6.15μm. Two types of polarization converter design are presented, with varying levels of fabrication difficulty and size considerations. The two types of polarization rotator, shown in Figs. 1(a) and (b), require one and two lithography steps respectively. However, as will be shown, the polarization rotator in Fig. 1(b) occupies much less space and is significantly more tolerant to fabrication variations.

We have experimentally demonstrated the operation of the one-step etch polarization rotator at λ=4.55μm in a SoS system [3, 4]. It relies on the conversion of TM0 to TE1 by gradually increasing the width of the waveguide. Once converted to TE1, the waveguide is split into 2 single mode waveguide arms that propagates TE0 components at 180-degree phase difference. A phase shifted is introduced as shown in one of the arms so that at the input of the 2×2 multimode interference (MMI) device, the TE0 waves are phase-shifted by 90-degree with respect to each other. An input TM0 will then be converted to TE0 that will be observed in the arm 1 as shown in the schematic. The device in Fig. 1(a) is in effect a polarization splitter rotator (PSR). The device sends an incoming TE0 wave as TE0 to arm 2 with minimum cross-talk in arm 1. For our case, we are interested in TM0 with output TE0 to arm 1.

Fig. 2(b) shows the plot of effective index (N_{eff}) versus waveguide width (w) of our structure shown in Fig. 1(a) for operation at λ=6.15μm. The epi structure comprises an InP substrate with 1.15μm InGaAs core, and a thin 0.55μm upper cladding of InP. The epi layers were chosen to optimize coupling from a monolithically grown and integrated QCL to the passive waveguides. As observed from Fig. 2(b), the transition from TM0 to TE1 occurs at approximately a waveguide width w=11μm. As observed from Fig. 2(c), 63% conversion efficiency is achieved over a length of 3.5mm. Obviously, if the converter length is increased, as shown by the blue curve, the conversion efficiency can be increased to above 80% at lengths greater than 5mm. It is also observed that the polarization rotator design is fabrication tolerant as shown by the selection of different widths of the pre-, post- and converter sections around a length of 2mm. Microscope image of a preliminary PSR device is shown in Fig. 1(c).

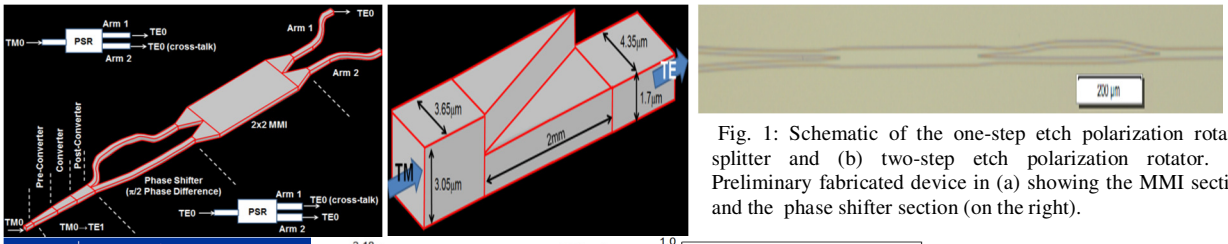

Fig. 1: Schematic of the one-step etch polarization rotator splitter and (b) two-step etch polarization rotator. (c) Preliminary fabricated device in (a) showing the MMI section and the phase shifter section (on the right).

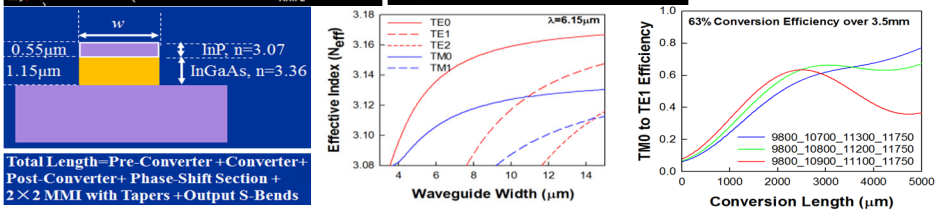

Fig. 2: (a) Effective Index versus width (w) of waveguide of the propagating waveguide modes simulated by finite-element modeling (FEM) for the waveguide epi structure in (b). TM0 to TE1 conversion occurs at w~11μm. The total TM1 to TE1 convertor comprises a pre-converter, a converter and post-converter. (c) shows TM0 to TE1 conversion efficiency versus width o f the converter section: for the red curve, pre-converter width changes from 9.8μm to 10.9μm over 1mm, pre-converter width changes from 10.9μm to 11.1μm over 2mm, post-converter width changes from 11.1μm to 11.75μm over 0.1mm. MMI length=435μm, MMI Width=22.7μm; The phase shifter is formed with waveguides of Bezier curves that gives the required π/2 phase shift between the two input arms of the 2×2 MMI. 63% conversion efficiency from TM0 to TE0 is achieved over a total length 3.5mm.

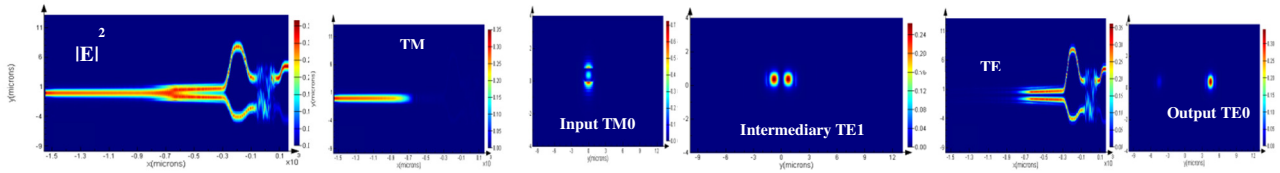

Fig. 3: Evolution of the mode from input TM0 to output TE0 via intermediate TE1

In the polarization rotator of Fig. 1(b), a dual etch processing is required [5]. However, this type of polarization rotator achieves direct conversion / rotation from TM0 to TE0 polarization and can be significantly more broadband than the single etch PSR. Fig. 4(b) and 4(c) show the corresponding epi profile at the input and output sections. As observed from Fig. 4(d), greater than 90% conversion efficiency is achieved for lengths greater than 2.5mm with nearly 99% achieved for a 5mm long taper. We observed that the polarization conversion efficiency is independent of the etch into the handle InP, for depths greater than 1μm. Hence a precise etch stop is not needed in this case. However, a precise etch stop is needed for the polarization rotator in Fig. 1(a) since efficiency drops significantly for etch depths greater than 200nm into the handle InP.

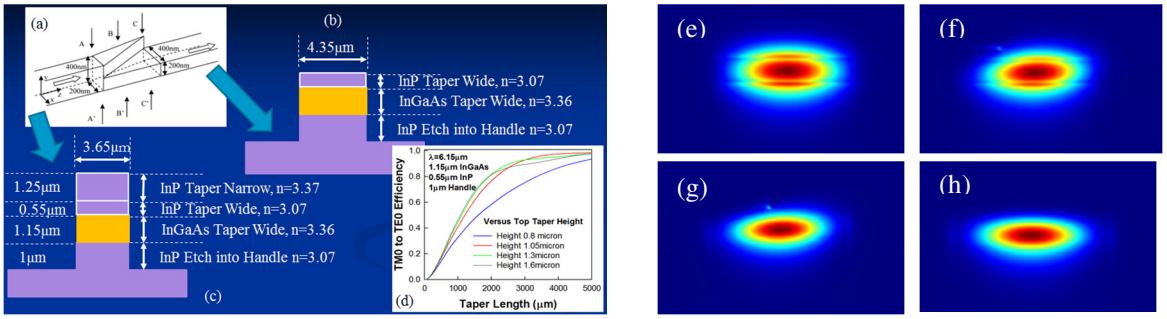

Fig. 4: (a) Schematic of the dual layer polarization rotator (b) and (c) shows the effective structure at the input and output sections. (d) shows TM0 to TE0 conversion efficiency for different heights of the top taper section that is etched away completely on the output end. We also consider that the structure is etched ~1μm into the handle. (e)-(h) shows the mode evolution from TM0 to TE0 at different sections.

Device fabrication has been completed. Measurements are in progress and will be presented. Designs presented here can be extended to any wavelength in the molecular fingerprint window from λ=3-15μm. The research was supported by Army (ARO) SBIR Contract #W911NF-17-P-0056. The content of the information does not necessarily reflect the position or the policy of the Government, and no official endorsement should be inferred

References

[1] CLEO Co-Submission (2018).
[2] Y. Zou et al., Sens. and Actuators B: Chemical 221, 1094 (2015)
[3] CLEO Co-Submission (2018).
[4] Y. Ding, H. Ou, C. Peucheret, Opt. Lett. 38 (8), 1227 (2013)
[5] J. Zhang, D-L. Kwong, et al., Opt. Express 18 (24), 25624 (2010)